HHS Public Access

Author manuscript

Cell Microbiol. Author manuscript; available in PMC 2020 February 01.

Published in final edited form as:

Cell Microbiol. 2019 February ; 21(2): e12992. doi:10.1111/cmi.12992.

Interferon-gamma production in Lyme arthritis synovial tissue promotes differentiation of fibroblast-like synoviocytes into immune effector cells

Robert B. Lochhead[1,†,*], **David Ordoñez**[1], **Sheila L. Arvikar**[1], **John M. Aversa**[2], **Luke S. Oh**[3], **Benton Heyworth**[4], **Ruslan Sadreyev**[5], **Allen C. Steere**[1], and **Klemen Strle**[1]

[1]Center for Immunology & Inflammatory Diseases, Division of Rheumatology, Allergy, & Immunology, Massachusetts General Hospital and Harvard Medical School, Boston, MA USA

[2]Department of Orthopedics, Yale University School of Medicine, New Haven, CT USA

[3]Department of Orthopedics, Massachusetts General Hospital and Harvard Medical School, Boston, MA USA

[4]Department of Orthopedics, Boston Children's Hospital and Harvard Medical School, Boston, MA USA

[5]Department of Molecular Biology and Department of Pathology, Massachusetts General Hospital and Harvard Medical School, Boston, MA USA.

Abstract

Lyme arthritis (LA), a late disease manifestation of *Borrelia burgdorferi* infection, usually resolves with antibiotic therapy. However, some patients develop proliferative synovitis lasting months to several years after spirochetal killing, called post-infectious LA. In this study, we phenotyped hematopoietic and stromal cell populations in the synovial lesion *ex vivo* and used these findings to generate an *in vitro* model of LA using patient-derived fibroblast-like synoviocytes (FLS). *Ex vivo* analysis of synovial tissue revealed high abundance of IFNγ-producing T cells and NK cells. Similar to marked IFNγ responses in tissue, post-infectious LA synovial fluid also had high levels of IFNγ. HLA-DR-positive FLS were present throughout the synovial lesion, particularly in areas of inflammation. FLS stimulated *in vitro* with *B. burgdorferi*, which were similar to conditions during infection, expressed 68 genes associated primarily with innate immune activation and neutrophil recruitment. In contrast, FLS stimulated with IFNγ, which were similar to conditions in the post-infectious phase, expressed >2000 genes associated with pathogen sensing, inflammation, and MHC Class II antigen presentation, similar to the expression profile in post-infectious synovial tissue. Furthermore, co-stimulation of FLS with *B. burgdorferi* and IFNγ induced greater expression of IL-6 and other innate immune response proteins and genes than with IFNγ stimulation alone. These results suggest that *B. burgdorferi* infection, in combination with IFNγ, initiates the differentiation of FLS into a highly inflammatory phenotype. We hypothesize that

*Corresponding author: rlochhead@mcw.edu (RBL).
†Current affiliation is The Department of Microbiology and Immunology, The Medical College of Wisconsin, Milwaukee, WI USA

CONFLICT OF INTEREST

None of the authors have any conflicts of interest to declare.

over-expression of IFNγ by lymphocytes within synovia perpetuates these responses in the post-infectious period, causing proliferative synovitis and stalling appropriate repair of damaged tissue.

INTRODUCTION

Lyme arthritis (LA) is the most common late-disease manifestation of *Borrelia burgdorferi* infection (Steere, Schoen, & Taylor, 1987). Most patients with LA resolve their arthritis with 1–2 months of oral antibiotic therapy and, if needed, with an additional month of IV antibiotic treatment. However, a subset of patients has persistent arthritis for months to several years after antibiotic therapy, referred to as post-infectious, antibiotic-refractory LA (Arvikar & Steere, 2015; Steere & Angelis, 2006).

During the infection, LA patients usually have marked elevations of white blood cells in their synovial fluid (SF), consisting primarily of polymorphonuclear (PMN) leukocytes, presumably directed against the pathogen (Lochhead et al., 2017). In patients with post-infectious LA, however, relative percentages of PMNs are lower, and percentages of mononuclear leukocytes and lymphocytes are higher, than in the infectious period. Patients with post-infectious LA also typically develop marked proliferative synovitis, which is greater than that during active infection. These differences between LA during the infectious versus the post-infectious phase are accompanied by distinct extracellular microRNA profiles in SF, showing that the nature of the arthritis is altered from an infection-induced inflammatory response to an immune-mediated inflammatory response (Lochhead et al., 2017).

The synovial lesion in post-infectious LA is characterized by a robust Th1 inflammatory signature, a marked interferon (IFN) expression profile and suppressed expression of genes associated with tissue repair (Lochhead et al., 2018). Consistent with this finding, high levels of Th1 cytokines and chemokines in SF, including IFNγ and IFNγ-inducible T cell chemokines CXCL9 and CXCL10, are particularly elevated (Shin, Glickstein, & Steere, 2007; Strle, Shin, Glickstein, & Steere, 2012; Strle et al., 2017), and CD4+ T cells from SF produce high levels of IFNγ when re-stimulated *in vitro* (Shen et al., 2010; Vudattu, Strle, Steere, & Drouin, 2013).

In *B. burgdorferi*-infected mice, robust IFN responses and suppressed tissue repair responses are found in joints of mouse strains that develop severe LA (Crandall et al., 2006). In particular, $Il10^{-/-}$ (C57BL/6) mice have a marked Th1 signature and over-production of arthritogenic IFNγ by T cells (Sonderegger et al., 2012; Whiteside et al., 2018). This Th1/IFNγ signature is sustained in joints of $Il10^{-/-}$ mice for up to 18 weeks post-infection, when *B. burgdorferi* are no longer detectible in joint tissue (Whiteside et al., 2018). Thus, in humans and in $Il10^{-/-}$ mice, excessive IFNγ responses may persist even after spirochetes are cleared from joint tissue.

Fibroblast-like synoviocytes (FLS) are the most abundant cell type in inflamed synovial tissue and are key effector cells in rheumatoid arthritis (RA) (Noss & Brenner, 2008; You, Koh, Leng, Kim, & Bucala, 2018). In RA, FLS are epigenetically altered and develop an oncogenic phenotype, resulting in chronic inflammation, proliferative synovitis, and joint

damage (Ai et al., 2018; Bottini & Firestein, 2013; Kasperkovitz et al., 2005). In *B. burgdorferi*-infected mice, synovial fibroblasts are a dominant source of IFN-inducible genes, such as T cell chemokines CXCL9 and CXCL10 (Lochhead et al., 2012; Paquette et al., 2017). This IFN profile is also associated with the suppressed tissue repair phenotype seen in mice with severe LA (Crandall et al., 2006). However, it is unknown what effect over-production of IFNγ has on FLS phenotype in LA pathogenesis.

In this study, characterization of cellular composition of synovial tissue demonstrated that T cells were the most abundant hematopoietic cell type in the post-infectious LA synovium. Moreover, multiple lymphocyte populations, including T cells and NK cells, were sources of IFNγ *ex vivo*. Importantly, FLS had a highly inflammatory phenotype and expressed very high levels of IFNγ-dependent MHC Class II HLA-DR molecules. In an *in vitro* model of LA using primary human FLS derived from post-infectious LA synovial tissue, IFNγ primed these stromal cells to become highly inflammatory and hyper-responsive to *B. burgdorferi* infection. These findings suggest that high levels of IFNγ produced by infiltrating lymphocytes during the infection drive FLS differentiation into highly inflammatory immune effector cells, rather than tissue-remodeling myofibroblast-like synoviocytes. This immune effector phenotype may persist if IFNγ responses are not down-regulated after infection, resulting in proliferative synovitis and stalled wound healing, which are hallmarks of post-infectious LA.

RESULTS

Patient characteristics

Fresh synovial tissue was available for assessment of lymphocyte subsets after enzymatic digestion of tissue from 3 patients with post-infectious LA who were seen in 2016–2017. Patients were treated for their LA with 1–4 months oral antibiotic therapy and 1 month of IV ceftriaxone. Following incomplete resolution of their arthritis after antibiotic therapy, 2 patients received disease modifying anti-rheumatic drug (DMARD) therapy for 6 or 21 months. Neither patient showed reactivation of infection with DMARD therapy, indicating their arthritis was no longer due to active *B. burgdorferi* infection. However, their arthritis did not fully resolve after DMARD therapy, and they underwent an arthroscopic synovectomy of the affected knee 14 or 44 months after completion of IV antibiotic therapy. The third patient, a 64-year-old woman with a history of degenerative arthritis, declined DMARD therapy and elected to have total knee replacement surgery 4 months after completion of IV ceftriaxone therapy. In each case, synovial tissue was collected and processed for analysis on the day of surgery.

Multiple lymphocyte subsets are sources of IFNγ in post-infectious LA synovial tissue

Transcriptome analysis of the synovial lesion identified a robust IFNγ expression profile as a key feature of post-infectious LA. These results are described in a companion article in this issue (Lochhead et al., 2018). In the current study, we assessed specific cellular sources of IFNγ in synovial tissue from patients with post-infectious LA and other forms of inflammatory arthritis. After enzymatic digestion, lymphocytes were isolated from fresh synovial tissue and analyzed by intracellular cytokine staining and flow cytometric analysis

to determine the cellular sources of IFNγ. In patients with post-infectious LA, T cells were the most abundant hematopoietic cell type in synovium, representing ~40–60% of total live cells isolated after tissue digestion (Fig 1a). CD3+ T cells consisted of 3 subsets: CD4+ T cells, CD8+ T cells, and CD4-CD8-CD3+ double-negative (DN) populations, the latter likely composed of a mixture of innate and adaptive T lymphocytes. NK cells were also present in synovial tissue and constituted 1–3% of total live cells. Subsets of CD4+, CD8+, and DN T cells, as well as CD56+ NK cells, were IFNγ-positive by intracellular cytokine staining (Fig 1b). Of note, staining was performed on cells in the absence of stimulation with PMA and ionomycin, indicating that these lymphocyte subsets were actively producing IFNγ at the time of synovectomy and cell isolation. Relatively fewer CD4+ T cells were IFNγ-positive, compared with CD8+ T cells, although overall there were higher numbers of CD4+ T cells in tissue. We previously showed that CD4+ and CD8+ T cells are the most abundant infiltrating cells in LA synovitis (Steere, Duray, & Butcher, 1988), and ~50% of CD4+ T cells collected *ex vivo* from synovial fluid were IFNγ-positive following restimulation with PMA and ionomycin (Vudattu et al., 2013). Together, these results indicate infiltrating T lymphocytes in post-infectious LA primarily consist of a Th1 effector phenotype.

For comparison, synovial tissue this analysis was also available from 2 patients with RA and one patient with ankylosing spondylitis (SpA). For these 3 patients, the tissue was obtained years after disease onset and treatment of their arthritis with DMARD therapy. In these patients, ~5–20% of total live cells isolated from tissue were T cells, which were significantly lower than that seen in post-infectious LA (Fig 1c). In addition to analysis of T cells and NK cells, sufficient numbers of cells were available for analysis of myeloid cell and B cell populations from synovial tissue from 2 patients with post-infectious LA, from 1 patient with RA, and from 1 patient with SpA (Fig 1c, Supplemental Fig S1). CD11b+ HLA-DR+ monocyte/macrophage populations were the most abundant myeloid cell type in these patients, and with the exception of the SpA patient, tissue from these patients contained low numbers of B cells (Fig. 1c). Thus, consistent with previous studies (Shen et al., 2010; Steere et al., 1988; Vudattu et al., 2013), we showed that T cells were the most abundant leukocyte population and multiple T cell subsets and NK cells were important sources of IFNγ in post-infectious LA synovial tissue. In contrast, patients with other forms of inflammatory arthritis had variable levels of T cells, myeloid cells, and B cells.

IFNγ and IFN-inducible chemokine CXCL10 are abundant in post-infectious LA synovial fluid

Although fresh synovial tissue was only available for cell analysis from 6 patients for this study, synovial fluid (SF) was available for cytokine analysis from larger numbers of patients. SF was obtained from 14 patients with LA who had all received 1–2 months oral and 1-month IV antibiotic therapy prior to sample collection and were well into the post-infectious phase. SF was collected a median of 8 months after arthritis onset (range=3–17 months), and total arthritis duration was 17 months (range=6–32 months). All 14 patients received DMARD therapy after sample collection, and 12 of the 14 patients resolved their arthritis following DMARDs, whereas 2 patients had incomplete responses to DMARD therapy and underwent synovectomies. As comparison groups, SF from 5 patients with early

RA (within 6 months of initial diagnosis), 7 with established RA (longer than 6 months from initial diagnosis), and 12 with osteoarthritis (OA) were also analyzed.

Post-infectious LA SF contained very high protein levels of IFNγ, the IFN-inducible T cell chemokine CXCL10, as well as the cytokines TNFα and IL-6, compared with SF from minimally inflammatory OA (Fig 2). In addition, LA SF contained modestly elevated levels of IL-12p40, IL-12p70, IL-17A, and IL-1β compared to OA SF, but these differences did not achieve statistical significance. In contrast, SF from early RA had higher proteins levels of IL-12p40, IFNγ, and CXCL10 than OA. Moreover, SF from established RA had higher IL-12p70, IFNγ, IL-17A, TNFα, and IL-1β levels than OA (Fig 2). Thus, in patients with post-infectious LA, the inflammatory environment in SF is characterized by strong Th1 responses, as reported previously (Gross, Steere, & Huber, 1998; Shin et al., 2007), though some patients have moderate Th17 responses as well (Shen et al., 2010). In contrast, both Th1 and Th17 inflammatory profiles are often observed in RA (McInnes & Schett, 2007).

Abundance of HLA-DR-positive fibroblast-like synoviocytes in synovial tissue

FLS are important sources of inflammatory cytokines and tissue-degrading proteases in RA (Bartok & Firestein, 2010) and in murine LA (Lochhead et al., 2012), and are the most abundant stromal cell type in synovium (You et al., 2018). To evaluate the phenotype of stromal cells in synovial tissue, isolation and staining of the non-hematopoietic (CD45-) cell lineages was performed. Endothelial cells (EC) were defined as CD45- CD31+, and FLS were CD45- CD31-CD90+. EC also expressed high levels of ICAM1 and VCAM1, and nearly all FLS were CD44+, ICAM1+, and VCAM1+ (Fig 3a), which has been shown previously by histologic analysis (Akin, Aversa, & Steere, 2001), indicating EC and FLS have an activated phenotype.

MHC Class II molecules, such as HLA-DR, may be expressed on activated stromal cells such as FLS and EC, which has been shown previously to be dependent on IFNγ-mediated upregulation of MHC Class II transactivator (CIITA) (Tran et al., 2007; Waldburger, Suter, Fontana, Acha-Orbea, & Reith, 2001). In RA, HLA-DR-positive FLS have been shown *in vitro* to function as nonprofessional antigen presenting cells (APC) (Tran et al., 2007). In post-infectious LA tissue, HLA-DR expression levels on FLS and EC populations were quite variable, whereas populations of CD45+ cells showed a clearly defined HLA-DR-positive population (presumably professional APCs) and an HLA-DR-negative population (Fig 3a). Similar variability in HLA-DR expression was observed in FLS and EC isolated from synovial tissue from other types of inflammatory arthritis (Fig 3b).

Localization of HLA-DR-positive FLS within synovial tissue

Archived tissue sections from synovial biopsies were available from 13 patients with post-infectious LA to determine localization of HLA-DR-positive FLS in synovial lesions. In these patients, synovial biopsies were collected during surgical procedures usually performed >1 year after completion of oral and IV antibiotic treatment for *B. burgdorferi* infection. Synovial biopsies from 2 patients with RA and 3 with OA were used as comparison groups. Immunofluorescence microscopy was employed to identify FLS that were positive for both vimentin (FLS marker) and HLA-DR (Fig 3c).

Tissue sections from patients with post-infectious LA had wide-spread HLA-DR expression throughout the tissue, particularly in areas of inflammation such as the synovial sublining and surrounding the inflamed microvasculature. Vimentin staining of FLS was seen throughout the synovium, as expected in this FLS-rich tissue. HLA-DR-positive vimentin-positive stromal cells (in yellow) were most commonly observed within the synovial sublining. These double-positive cells were also observed in areas surrounding the vasculature, which may be a mixture of HLA-DR-positive FLS and HLA-DR-positive vimentin-positive endothelial cells (examples shown in Fig 3c).

To compare these findings in multiple patients, semi-quantitative analysis of HLA-DR and vimentin colocalization was conducted for each section. Green fluorescence (HLA-DR), red fluorescence (vimentin), and yellow fluorescence (double positive, DP) intensity were quantified from 3 separate 20× frames per sample (Fig 3c). Approximately 45% of HLA-DR expression overlapped with vimentin, indicating FLS were major contributors of HLA-DR expression within inflamed synovial tissue. Sections from patients with RA and OA had similar findings, indicating that this may be an inherent feature of damaged or inflamed synovium (Fig 3c).

FLS stimulated *in vitro* with *B. burgdorferi* and IFNγ have dramatically altered gene expression profiles

In an effort to recapitulate the effects of IFNγ on FLS during the infectious and post-infectious phases of LA, we developed an *in vitro* model of LA using primary human FLS. For this study, FLS cell lines derived from 5 post-infectious LA patients were stimulated with *B. burgdorferi* (10:1 MOI), IFNγ (20 ng/ml), or *B. burgdorferi* + IFNγ for 16 hours (Fig 4). These three stimuli mimic 3 distinct *in vivo* conditions: 1: infection with *B. burgdorferi* in the absence of IFNγ stimulation (FLS+*B. burgdorferi*); 2: infection with *B. burgdorferi* accompanied by excessive IFNγ/Th1 responses (FLS+*Bb* and IFNγ); and 3: chronic IFNγ/Th1 responses in the absence of active infection (FLS+IFNγ).

Transcriptomic analysis of *B. burgdorferi*-stimulated FLS identified 68 genes that were differentially expressed compared with unstimulated FLS. Stimulation with IFNγ had a much more pronounced effect on the FLS transcriptome, with 2,246 differentially expressed genes. However, the most pronounced effect on FLS expression was stimulation with both *B. burgdorferi* and IFNγ, resulting in 3,254 differentially expressed genes. Thus, > 1,200 genes were uniquely expressed in the *B. burgdorferi* + IFNγ stimulated FLS, compared with stimulation with either *B. burgdorferi* or IFNγ alone (complete gene list in Supplemental Table S1).

Gene expression profiles in IFNγ-stimulated FLS is similar to expression profiles in post-infectious LA synovial tissue

Transcriptional profiling of differentially expressed genes in stimulated versus unstimulated FLS was performed using KEGG pathway analysis (Fig 5). In FLS stimulated with *B. burgdorferi* alone, the 68 differentially-expressed genes included those associated with immune disorders, inflammatory pathways, and infectious diseases (Fig 5a). These results

were similar to a previously published report using dermal fibroblasts stimulated with various *Borrelia* strains (Meddeb et al., 2016).

In FLS stimulated with IFNγ, the 2,246 differentially-expressed genes included those associated with chronic inflammatory and autoimmune disorders, infectious diseases, and cancer, which were up-regulated; and pathways associated with cell metabolism, cell cycle regulation, and amino acid biosynthesis, which were down-regulated (Fig 5b). FLS stimulated with both *B. burgdorferi* and IFNγ had an expression profile similar to IFNγ alone, albeit somewhat more expanded, particularly in the up-regulation of cancer-associated pathways, consistent with oncogenic-like properties of activated FLS seen in RA (You et al., 2018). Importantly, the expression profile of FLS stimulated with IFNγ or IFNγ+*B. burgdorferi* in cell culture was remarkably similar to the expression profile of post-infectious LA synovial tissue, including pathways involved in antigen processing and presentation, NF-kappa B signaling, and innate sensing pathways, as shown in a companion article in this issue (Lochhead et al., 2018).

Synergistic effects of *B. burgdorferi* and IFNγ on FLS expression of inflammatory mediators

Gene expression results demonstrated that co-stimulation of FLS with IFNγ and *B. burgdorferi*, which simulates pro-arthritogenic inflammatory conditions during infection, had synergistic rather than additive effects on FLS activation, compared with stimulation with *B. burgdorferi* or IFNγ alone, which simulates inflammatory conditions in the post-infectious LA phase (gene list in Supplemental Table S1).

Differential expression analysis identified 105 genes upregulated in FLS stimulated with IFNγ+*B. burgdorferi*, compared with IFNγ stimulation alone (Fig 6a). KEGG analysis revealed that among these 105 genes, 32 were associated with innate immune activation (i.e., TNF, pathogen recognition receptor (PRR), and NF-kappa B signaling pathways). Hierarchical clustering analysis of these genes using Morpheus (Broad Institute) separated gene expression into 3 clusters (Fig 6a). The first group of genes were those dependent on *B. burgdorferi* stimulation, which included CXC-motif neutrophil chemokines, fibroblast collagenase (MMP1), and innate cytokines IL1B and TNF. The second cluster of genes were those dependent on IFNγ which were amplified with IFNγ+*B. burgdorferi* stimulation. These included T cell chemokines (CXCL10, CXCL11, and CX3CL1), adhesion molecule ICAM1, NF-kappa B transcription factor RELA, and nitrous oxide synthase (NOS2). The third cluster of genes were those that were modestly upregulated in FLS stimulated with either *B. burgdorferi* or IFNγ, but markedly elevated when FLS were stimulated with both. These included genes associated with inflammatory cytokines such as IL6 and those associated with PRR/NF-kappa B/MAP kinase signaling (i.e., MAP3K8, NFKB1/2, NOD2, TNFAIP3, etc.), as well as the anti-apoptotic gene BIRC3 and transcription factor JUNB.

Analysis of protein levels of cytokines produced by stimulated FLS also showed distinct expression profiles between groups (Fig 6b). Compared with unstimulated cells, IL-6 was modestly up-regulated with *B. burgdorferi* or IFNγ stimulation alone, although these differences did not achieve statistical significance. In contrast, FLS stimulated with both *B. burgdorferi* and IFNγ secreted very high levels of IL-6. Secretion of the neutrophil

chemokine IL-8, however, appeared to be completely dependent on *B. burgdorferi* stimulation, and IFNγ had little effect on IL-8 production. Finally, secretion of monocyte chemoattractant protein 1 (CCL2) and Th1-associated chemokines CXCL9 and CXCL10 were most strongly elevated in FLS following IFNγ stimulation. These *in vitro* cytokine expression findings indicate that FLS are likely important in determining which immune cells are recruited to joints during infection, when SF contains primarily neutrophils, and during the post-infectious phase, when SF contains relatively fewer PMNs and relatively more mononuclear cells and lymphocytes (Lochhead et al., 2017). Furthermore, the cytokine profile in FLS stimulated with both *B. burgdorferi* and IFNγ was similar to our previous reports of cytokine secretion by myeloid cells from LA patients stimulated with *B. burgdorferi*, most notably the inflammatory cytokine IL-6 (Shin et al., 2007), indicating that the cytokine profile of these activated FLS may be phenotypically analogous to M1-like macrophages.

FLS expression of MHC Class II antigen presenting genes

Stimulation of FLS with IFNγ or IFNγ+*B. burgdorferi* also resulted in strong upregulation of a large number of genes associated with antigen presentation, including CIITA, MHC Class I and Class II molecules, and other associated genes (Fig 6c). To determine whether HLA-DR molecules were expressed on the cell surface, FLS were stimulated with *B. burgdorferi*, IFNγ, or both. Flow cytometric analysis demonstrated that HLA-DR was surface-expressed in an IFNγ-dependent manner (Fig 6d). These results are consistent with phenotypic analysis of FLS isolated directly from fresh synovial tissue (Fig 3a) and immunofluorescence microscopic analysis of synovial biopsies (Fig 3c). Thus, as shown with both *ex vivo* and *in vitro* analyses, IFNγ appears to induce the differentiation of FLS into HLA-DR+ stromal cells (i.e., nonprofessional APCs) within the post-infectious LA synovial lesion.

DISCUSSION

Expression analysis of synovial tissue performed in a parallel study demonstrated excessive expression of IFNγ-responsive genes as a defining characteristic of post-infectious LA (Lochhead et al., 2018). In this study, we found that multiple lymphocyte subsets within synovial tissue contributed to this robust IFNγ profile, including CD4+ T cells, cytotoxic CD8+ T cells, double-negative T cells, and NK cells. In contrast, cells and inflammatory cytokines from patients with other forms of inflammatory arthritis were more varied, likely reflecting variability in disease etiology, arthritis duration, and pathogenic mechanisms. Thus, post-infectious LA appears to be most strongly associated with a marked IFNγ response in synovial tissue, involving a broad range of IFNγ-producing cell populations in humans.

Similar to our findings in patients with post-infectious LA, a recent study using the IL-10 knockout mouse model of persistent LA demonstrated that the arthritis is caused by dysregulated IFNγ production by CD4+ and CD8+ T cells in a TLR2-dependent manner (Whiteside et al., 2018). Furthermore, in this model, T cells are activated during the initial stages of arthritis development when spirochetes are present in joints, and remain activated

for at least 18 weeks, even when spirochetes are no longer detectible in joint tissue (Whiteside et al., 2018). Although the $Il10^{-/-}$ murine LA model may not fully recapitulate post-infectious LA in humans, these animal studies also demonstrate the persistence of arthritogenic responses in the post-infectious period.

Although wild-type mice resolve their arthritis with antibiotic therapy, the $Il10^{-/-}$ mouse model of IFNγ-dependent LA is the closest equivalent to human post-infectious LA, in which IFNγ, rather than *Borrelia* infection, appears to play a central role in pathogenesis (Lochhead et al., 2018). In both $Il10^{-/-}$ mice (Whiteside et al., 2018) and patients with post-infectious LA (Lochhead et al., 2018), IFNγ responses persist or worsen, despite undetectable pathogen loads (Li et al., 2011). These results suggest that impaired or inadequate IL-10 responses during and/or after infection may play a role in human post-infectious LA pathogenesis. Indeed, most $CD4+CD25^{high}$ T cells in SF from patients with post-infectious LA, which are ordinarily a regulatory phenotype, secrete large amounts of TNFα and IFNγ, consistent with Th1 effector phenotype, and relatively few secrete IL-10. These cells fail to suppress Th1 responses *in vitro* (Vudattu et al., 2013). Here, we extend these findings by showing that in addition to CD4+ T cells, multiple lymphocyte populations contribute to IFNγ production and dysregulated immune responses.

The pronounced IFNγ profile in synovial tissue correlated strongly with suppressed expression of genes associated with tissue repair and wound healing. Stromal cells, particularly fibroblasts and endothelial cells, are the major cell types involved in the repair of damaged tissue and production of extracellular matrix. Importantly, we found that these cell types were highly activated in post-infectious LA synovial tissue, consistent with our previous findings in mice which showed that fibroblasts and endothelial cells are important producers of arthritogenic cytokines and chemokines in LA (Lochhead et al., 2012). The polarization of FLS towards a highly inflammatory phenotype may impair their ability to repair damaged tissue, thereby contributing to pathogenesis of the lesion.

Expression of HLA-DR molecules by activated FLS indicated that these stromal cells may be acting as nonprofessional APCs and altering T cell responses within inflamed synovial tissue in LA. There is precedent for HLA-DR+ FLS functioning as nonprofessional APCs in RA, the prototypic joint autoimmune disease. FLS from RA patients express HLA-DR molecules and inflammatory cytokines when stimulated by IFNγ or IL-17-producing T cells (Kato, Endres, & Fox, 2013), and these HLA-DR-positive FLS can present immunogenic autoantigens to T cells (Carmona-Rivera et al., 2017; Tran et al., 2007). In RA, HLA-DR+ FLS express an altered repertoire of B7 family costimulatory molecules, compared with myeloid-derived professional APCs, and appear to have both stimulatory and inhibitory effects on various T cell subsets (Tran et al., 2008). Our results suggest that in LA, IFNγ is the primary effector cytokine in shaping FLS activation, whereas in RA, both IFNγ and IL-17 may promote FLS activation.

Based on an analysis of HLA-DR-presented peptides in LA synovial tissue (Wang et al., 2017), we previously identified 4 LA-associated autoantigens: endothelial cell growth factor, matrix metalloproteinase-10, apolipoprotein B-100, and annexin A2 (Crowley et al., 2015; Crowley et al., 2016; Drouin et al., 2013; Pianta et al., 2015). These 4 self-proteins are

abundant in post-infectious LA synovial tissue and are involved in tissue damage and/or wound repair. During both active infection and in the post-infectious LA phase, subsets of patients have autoantibody responses to one or more of these autoantigens; and in the post-infectious phase, these autoantibodies correlate with specific aspects of synovial histology (Sulka et al., 2018). Moreover, patients with post-infectious LA often develop autoreactive T cell responses, and it is still unclear why the IFNγ-producing T cells are abundant in synovial tissue during the post-infectious phase, when spirochetes are no longer present, or whether these autoimmune responses have a role in perpetuating the disease. Therefore, it will be important to determine whether HLA-DR+ FLS are contributing to tissue-specific T cell responses, both during infection and in the post-infectious phase.

As part of this study, we developed an *in vitro* model of LA using primary human FLS derived from post-infectious LA patients stimulated with *B. burgdorferi* and/or IFNγ. This model appeared to recapitulate the excessive inflammatory conditions during infection (*B. burgdorferi*+ IFNγ) and during post-infectious LA (IFNγ alone). These *in vitro* studies demonstrated that FLS dramatically alter their phenotype when induced by high levels of IFNγ during *B. burgdorferi* infection, compared with activation during infection without IFNγ priming. Furthermore, if IFNγ responses are not resolved after spirochetal killing, FLS maintain high expression of adaptive immune genes, including those associated with T lymphocyte activation.

The gene expression profile in cultured FLS stimulated with IFNγ was quite similar to that seen in post-infectious LA synovial tissue (Lochhead et al., 2018). Notably, pathways associated with antigen processing and presentation, innate sensing, and T cell stimulation were markedly up-regulated both in IFNγ-stimulated FLS and in post-infectious LA patient tissue. This confirms the central role of IFNγ and FLS in LA pathogenesis and suggests that excessive IFNγ during infection could set the stage for persistent synovitis, even after *B. burgdorferi* have been cleared by antibiotics and the host immune response. It is likely that host and pathogen genetic factors contribute to this outcome. For example, patients with a TLR1 polymorphism (1805GG), which is found in ~50% of the European Caucasian population, have greater IFNγ responses to *B. burgdorferi*, and are more likely to develop post-infectious LA (Strle et al., 2012).

We postulate the following sequence of events in the pathogenesis of post-infectious LA. During active infection, the host response to *B. burgdorferi* in joints results in synovial inflammation and tissue damage, which must be repaired following pathogen clearance. FLS are a key effector cell type in these processes. During infection, they facilitate tissue-specific immune activation against the pathogen, and following bacterial clearance, facilitate resolution of immune responses and initiation of tissue repair. FLS respond to infiltrating *B. burgdorferi* by producing innate cytokines and chemokines that recruit leukocytes, particularly PMNs, which aid in the elimination of pathogen. As the infection is controlled, FLS normally mature into tissue-forming myofibroblasts and promote repair of damaged tissue. We suspect that anti-inflammatory responses, such as regulatory T cell activation and IL-10 secretion, are necessary to suppress innate and Th1 responses, thereby allowing transition from anti-bacterial immune responses to initiation of tissue repair and wound healing.

Under pathogenic conditions, dysregulated IFNγ responses, likely initiated during infection, lead to pathogenic activation of FLS, which differentiate into potent immune effector cells. These FLS are highly responsive to IFNγ and pathogen-derived inflammatory stimuli and produce excessive amounts of innate and adaptive cytokines and chemokines, including the T cell chemoattractant CXCL9 and CXCL10. This results in ongoing recruitment of IFNγ-producing T and NK cells, perpetuating the pro-inflammatory FLS phenotype. Lymphocytes remain activated in the inflamed synovium, even after spirochetes are no longer present, presumably due to unresolved autoimmune responses (Crowley et al., 2015; Crowley et al., 2016; Drouin et al., 2013; Pianta et al., 2015) and/or through bystander activation of infiltrating T cells (Whiteside et al., 2018). Under these chronic conditions, FLS may provide co-stimulatory signals to infiltrating lymphocytes and produce tissue-damaging proteases and inflammatory molecules, thereby blocking appropriate repair of damaged tissue. The result is persistent autoimmune/autoinflammatory responses, proliferative synovitis, and fibrosis, which are hallmarks of post-infectious LA.

MATERIALS AND METHODS

Ethics Statement

The study “Immunity in Lyme arthritis” was approved by the Human Investigations Committee at Massachusetts General Hospital (MGH), according to principles for medical research involving human subjects expressed in the World Medical Association Declaration of Helsinki. Written informed consent was obtained from all participants 18 years of age or older, or from patient and a parent or guardian of those between the ages of 12 and 17.

Patients

All patients with Lyme disease met the Centers for Disease Control and Prevention criteria for *B. burgdorferi* infection (Centers for Disease & Prevention, 1995), and those with RA, SpA, or OA met validated criteria for those diseases (Aletaha et al., 2010). All LA patients had swollen knees and high IgG antibody responses to *B. burgdorferi*, as determined by ELISA and Western blot. LA patients received treatment according to an algorithm (Steere & Angelis, 2006), as mentioned in the guidelines of the Infectious Diseases Society of America (Wormser et al., 2006).

Flow cytometric analysis of cell populations in synovial tissue

Fresh synovial tissue was collected from 3 post-infectious LA patients on the day of surgery. 3 or 4 randomly sampled ~100 mg pieces of finely-minced synovial tissue were incubated for 30 minutes in RPMI (Gibco) + 0.2 mg/ml Liberase TL (Roche) and 1 U/ml RNase-free DNase 1 (Novagen) at 37° C, gently agitating the media every 10 minutes. Digested tissue was filtered using a 100-micron mesh, red blood cells were lysed with ACK lysing buffer (Gibco), tissue-isolated cells were washed in phosphate-buffered saline (PBS), and re-suspended in fetal bovine serum (FBS) + 10% DMSO for storage in liquid nitrogen. Cells were washed for 10 min at 1000rpm in PBS + 1% FBS. Cells were re-suspended in 500 μl of PBS (without FBS) + 0.5% of Zombie UV Fixable Viability Dye (BioLegend) and incubated for 30–45 min at room temperature in the dark. After washing with 10 ml PBS, cells were incubated in the dark for 10 min at room temperature in 500 μl of a solution containing PBS

+ 1% FBS and 2% mouse serum (Sigma) to block any non-specific binding prior to staining with conjugated antibodies. The antibody cocktail for the lymphocyte panel included CD56-BV421, CD3-BV510, CD4-PE/Cy5 and CD8-APC/Cy7 to define NK cells and CD4, CD8 and double negative T cells. Stromal cell panel included CD105-PerCP/Cy5.5, CD54-PE, CD31-PE/Cy7, CD44-BV421, CD90-BV510, CD45-APC, and HLA-DR-Alexa Fluor 700. Myeloid cell panel included lineage (lin) cocktail (CD3/19/20/56)-APC, CD11b-PE, HLA-DR-Alexa Fluor-700, CD16-BV510, CD11c-BV605, and CD123-PerCP/Cy5.5. B lymphocyte panel included CD3-BV510, CD19-APC, CD27-PE, CD20-APC/Cy7, CD138-BV421, and CD38-BV711. All antibodies were from BioLegend, except for HLA-DR-Alexa Fluor-700 and CD11b-PE (BD Biosciences), and CD11c-PE/Cy7 (eBioscience). For surface staining, cells were incubated with the antibody mix for 10 min at room temperature in the dark. Intracellular cytokine staining was performed using anti-human IFNγ-PerCP/Cy5.5 and corresponding isotype control. Following surface staining of lymphocytes, cells were fixed and permeabilized with the Intracellular Fixation and Permeabilization Buffer Set (BioLegend), following the manufacturer instructions, and incubated with anti-IFNγ or isotype antibody for 25 min in the dark. Stained cells were then washed two times with PBS + 1% FBS to remove any remaining antibody and resuspended in FACS buffer for acquisition using an LSR Fortessa X-20 5-laser cell analyzer (Beckton Dickinson). Flow data were analyzed using FlowJo software (v.7.6.5).

Quantification of cytokines and chemokines in synovial fluid

Levels of 22 innate, Th1 and Th17 cytokines and chemokines were assessed in synovial fluid from 14 patients with post-infectious LA, 5 patients with early RA (<6 months from disease onset), established RA (>6 months from disease onset), and 12 patients with OA. Fluid was diluted 5-fold with PBS, and the levels of each mediator were assessed in one complete experiment using bead-based multiplex assays (EMD-Millipore) coupled with a Luminex-200 System Analyzer (Luminex).

Immunofluorescence microscopy

Synovial biopsies from 13 patients with post-infectious LA, which had been previously collected at the time of surgery, were immediately flash-frozen in optimal cutting temperature (OCT) medium and stored in liquid nitrogen. Two sections from each biopsy were stained with Vimentin-Alexa Fluor 647and HLA-DR-Alexa Fluor 488. Imaging was performed using a Zeiss LSM 780 confocal microscope. Semi-quantitative analysis of HLA-DR and vimentin staining was conducted for each biopsy. Green fluorescence (HLA-DR), red fluorescence (vimentin), and yellow fluorescence (co-localized green and red fluorescence) intensity was calculated in 3 20× frames from each sample using Zen Black software (Zeiss).

Isolation and culturing of primary FLS

FLS were derived from synovial tissue from 5 patients with post-infectious LA that was removed during arthroscopic synovectomy. Following surgery, tissue (~1g) was minced mechanically and then digested enzymatically by incubation in DMEM medium + 1mg/ml Collagenase Type 4 for 2h at 37°C (Viatte et al., 2015). Tissue homogenate was passed through a 70μm cell strainer and rinsed in PBS by centrifugation. After washing, cells were

resuspended in DMEM culture media + 10% FBS, L-glutamine, essential amino acids, non-essential amino acids, 2-mercaptoethanol, and antibiotics. Cells were cultured for 3 passages to obtain pure FLS cell line. FLS passage 3–7 were used for these experiments.

Borrelia burgdorferi culture

B. burgdorferi isolates (RST1, OspC type A) were recovered from an EM skin lesion of a patient in the Northeastern US. The isolate was grown to mid-log phase in complete Barbour-Stoenner-Kelly medium (Sigma Aldrich) containing 6% rabbit serum. In preparation for co-culture experiments with FLS, the spirochetes were washed in DMEM cell culture medium to remove confounding effects of growth factors. Spirochetes were enumerated by optical density using a carefully generated standard curve. The same *B. burgdorferi* isolate was used in all experiments.

FLS stimulation and RNA purification

FLS (2×10^5 cells/well) from 5 patients were each stimulated with a *B. burgdorferi* RST1 OspC type A strain at a multiplicity of infection (MOI) of 25 organisms per cell, IFNγ (10 ng/ml), or both for 16 hours, or left unstimulated. Cell supernatant was collected and stored at −80° C for cytokine analysis. Cells were washed 3× in ice-cold PBS. Approximately 100 ng total RNA was recovered from stimulated FLS using an RNeasy kit (Qiagen). NEBNext Poly(A) Ultra Directional processing kit (New England Biolabs) was used to separate mRNA from rRNA. FLS RNA quality was determined using a Bioanalyzer (Agilent), and low-quality RNA samples were excluded from this study. For flow cytometric analysis of stimulated FLS, cells were stained as above using CD44-BV421, CD90-BV510, HLA-DR-Alexa Fluor 700, with the respective isotype controls.

High-throughput RNA sequencing

RNA libraries were constructed using the NEBNext Ultra RNA Prep Kit for Illumina (New England Biolabs). Libraries were sequenced to a depth of ~25 million paired-end, 100 base-pair reads (Hi-Seq PE100 Reagent Kit, Illumina). Library preparation, sequencing, and bioinformatics were performed by the MGH NextGen Sequencing and Bioinformatics Core Facilities.

Bioinformatics analysis of gene expression

Copies per million reads (CPMR) were used to normalize expression between samples. The following web-based bioinformatics tools were used for gene expression analysis: Database for Annotation, Visualization, and Integrated Discovery v.6.8 (Huang da, Sherman, & Lempicki, 2009), a functional annotation tool; Morpheus (Broad Institute, software.broadinstitute.org/morpheus/), a matrix visualization and analysis platform; and Kyoto Encyclopedia of Genes and Genomes (KEGG) pathway analysis (GenomeNet, www.genome.jp/kegg/pathway) (Kanehisa & Goto, 2000), a tool to identify enriched biological pathways.

Cytokine secretion assay

Cell supernatants were collected from stimulation of FLS, as described above. Protein levels of chemokines (IL-8, CCL2, CCL3, CCL4, CXCL9 and CXCL10) and cytokines (TNF, IL-1β, IL-6, IL-10, IFNγ and IFNα) were determined in cell culture supernatants (1:25 dilution) using bead-based multiplex assays (EMD-Millipore) coupled with a Luminex-200 System Analyzer (Luminex).

Statistical analysis

Differential expression analysis (custom bioinformatics R script) was used to determine differences in mRNA expression, adjusting for false discovery error using Benjamini-Hochburg correction (adjusted p-value <0.05). Clustering of genes was performed using one minus Pearson correlation analysis. Other statistical analyses were performed as described in the Figure legends using PRISM v7 (Graph Pad).

Supplementary Material

Refer to Web version on PubMed Central for supplementary material.

REFERENCES

Ai R, Laragione T, Hammaker D, Boyle DL, Wildberg A, Maeshima K, … Firestein GS (2018). Comprehensive epigenetic landscape of rheumatoid arthritis fibroblast-like synoviocytes. Nat Commun, 9(1), 1921. doi:10.1038/s41467-018-04310-9 [PubMed: 29765031]

Akin E, Aversa J, & Steere AC (2001). Expression of adhesion molecules in synovia of patients with treatment-resistant Lyme arthritis. Infect Immun, 69(3), 1774–1780. doi:10.1128/IAI.69.3.1774-1780.2001 [PubMed: 11179355]

Aletaha D, Neogi T, Silman AJ, Funovits J, Felson DT, Bingham CO, 3rd, … Hawker G (2010). 2010 Rheumatoid arthritis classification criteria: an American College of Rheumatology/European League Against Rheumatism collaborative initiative. Arthritis Rheum, 62(9), 2569–2581. doi:10.1002/art.27584 [PubMed: 20872595]

Arvikar SL, & Steere AC (2015). Diagnosis and treatment of Lyme arthritis. Infect Dis Clin North Am, 29(2), 269–280. doi:10.1016/j.idc.2015.02.004 [PubMed: 25999223]

Bartok B, & Firestein GS (2010). Fibroblast-like synoviocytes: key effector cells in rheumatoid arthritis. Immunol Rev, 233(1), 233–255. doi:10.1111/j.0105-2896.2009.00859.x [PubMed: 20193003]

Bottini N, & Firestein GS (2013). Duality of fibroblast-like synoviocytes in RA: passive responders and imprinted aggressors. Nat Rev Rheumatol, 9(1), 24–33. doi:10.1038/nrrheum.2012.190 [PubMed: 23147896]

Carmona-Rivera C, Carlucci PM, Moore E, Lingampalli N, Uchtenhagen H, James E,… Kaplan MJ (2017). Synovial fibroblast-neutrophil interactions promote pathogenic adaptive immunity in rheumatoid arthritis. Sci Immunol, 2(10). doi:10.1126/sciimmunol.aag3358

Centers for Disease, C., & Prevention. (1995). Recommendations for test performance and interpretation from the Second National Conference on Serologic Diagnosis of Lyme Disease. MMWR Morb Mortal Wkly Rep, 44(31), 590–591. [PubMed: 7623762]

Crandall H, Dunn DM, Ma Y, Wooten RM, Zachary JF, Weis JH, … Weis JJ (2006). Gene expression profiling reveals unique pathways associated with differential severity of Lyme arthritis. J Immunol, 777(11), 7930–7942.

Crowley JT, Drouin EE, Pianta A, Strle K, Wang Q, Costello CE, & Steere AC (2015). A Highly expressed human protein, apolipoprotein B-100, serves as an autoantigen in a subgroup of patients With Lyme disease. J Infect Dis, 272(11), 1841–1850. doi:10.1093/infdis/jiv310

Crowley JT, Strle K, Drouin EE, Pianta A, Arvikar SL, Wang Q, … Steere AC (2016). Matrix metalloproteinase-10 is a target of T and B cell responses that correlate with synovial pathology in patients with antibiotic-refractory Lyme arthritis. J Autoimmun, 69, 24–37. doi:10.1016/j.jaut.2016.02.005 [PubMed: 26922382]

Drouin EE, Seward RJ, Strle K, McHugh G, Katchar K, Londono D, … Steere AC (2013). A novel human autoantigen, endothelial cell growth factor, is a target of T and B cell responses in patients with Lyme disease. Arthritis Rheum, 65(1), 186–196. doi:10.1002/art.37732 [PubMed: 23044924]

Gross DM, Steere AC, & Huber BT(1998). T helper 1 response is dominant and localized to the synovial fluid in patients with Lyme arthritis. J Immunol, 760(2), 1022–1028.

Huang da W, Sherman BT, & Lempicki RA (2009). Systematic and integrative analysis of large gene lists using DAVID Diomformatics resources. Nat Protoc, 4(1), 44–57. doi:10.1038/nprot.2008.211 [PubMed: 19131956]

Kanehisa M, & Goto S (2000). KEGG: kyoto encyclopedia of genes and genomes. Nucleic Acids Res, 28(1), 27–30. [PubMed: 10592173]

Kasperkovitz PV, Timmer TC, Smeets TJ, Verbeet NL, Tak PP, van Baarsen LG, … Verweij CL (2005). Fibroblast-like synoviocytes derived from patients with rheumatoid arthritis show the imprint of synovial tissue heterogeneity: evidence of a link between an increased myofibroblast-like phenotype and high-inflammation synovitis. Arthritis Rheum, 52(2), 430–441. doi:10.1002/art.20811 [PubMed: 15692990]

Kato H, Endres J, & Fox DA (2013). The roles of IFN-gamma versus IL-17 in pathogenic effects of human Th17 cells on synovial fibroblasts. Mod Rheumatol, 23(6), 1140–1150. doi:10.1007/s10165-012-0811-x [PubMed: 23306426]

Li X, McHugh GA, Damle N, Sikand VK, Glickstein L, & Steere AC (2011). Burden and viability of *Borrelia burgdorferi* in skin and joints of patients with erythema migrans or Lyme arthritis. Arthritis Rheum, 63(8), 2238–2247. doi:10.1002/art.30384 [PubMed: 21590753]

Lochhead RB, Arvikar SL, Aversa JM, Sadreyev RI, Strle K, & Steere AC (2018). Robust interferon signature and suppressed tissue repair gene expression in synovial tissue from patients with post-infectious, *Borrelia* burgdorferi-induced Lyme arthritis. Cell Microbiol, e12954. doi:10.1111/cmi.12954 [PubMed: 30218476]

Lochhead RB, Sonderegger FL, Ma Y, Brewster JE, Cornwall D, Maylor-Hagen H,… Weis JJ (2012). Endothelial cells and fibroblasts amplify the arthritogenic type I IFN response in murine Lyme disease and are major sources of chemokines in *Borrelia burgdorferi-infected* joint tissue. J Immunol, 789(5), 2488–2501. doi:10.4049/jimmunol.1201095

Lochhead RB, Strle K, Kim ND, Kohler MJ, Arvikar SL, Aversa JM, & Steere AC (2017). MicroRNA expression shows inflammatory dysregulation and tumor-like proliferative responses in joints of patients with post-infectious Lyme arthritis. Arthritis Rheumatol, 69(5), 1100–1110. doi:10.1002/art.40039 [PubMed: 28076897]

McInnes IB, & Schett G (2007). Cytokines in the pathogenesis of rheumatoid arthritis. Nat Rev Immunol, 7(6), 429–442. doi:10.1038/nri2094 [PubMed: 17525752]

Meddeb M, Carpentier W, Cagnard N, Nadaud S, Grillon A, Barthel C, … Schramm F (2016). Homogeneous inflammatory gene profiles induced in human dermal fibroblasts in response to the three main species of *Borrelia burgdorferi* sensu lato. PLoS One, 77(10), e0164117. doi:10.1371/joumal.pone.0164117

Noss EH, & Brenner MB (2008). The role and therapeutic implications of fibroblast-like synoviocytes in inflammation and cartilage erosion in rheumatoid arthritis. Immunol Rev, 223, 252–270. doi:10.1111/j.1600-065X.2008.00648.x [PubMed: 18613841]

Paquette JK, Ma Y, Fisher C, Li J, Lee SB, Zachary JF, … Weis JJ (2017). Genetic control of Lyme arthritis by *Borrelia burgdorferi* arthritis-associated locus 1 is dependent on localized differential production of IFN-beta and requires upregulation of myostatin. J Immunol, 799(10), 3525–3534. doi:10.4049/jimmunol.1701011

Pianta A, Drouin EE, Crowley JT, Arvikar S, Strle K, Costello CE, & Steere AC (2015). Annexin A2 is a target of autoimmune T and B cell responses associated with synovial fibroblast proliferation in patients with antibiotic-refractory Lyme arthritis. Clin Immunol, 760(2), 336–341. doi:10.1016/j.clim.2015.07.005

Shen S, Shin JJ, Strle K, McHugh G, Li X, Glickstein LJ, … Steere AC (2010). Treg cell numbers and function in patients with antibiotic-refractory or antibiotic-responsive Lyme arthritis. Arthritis Rheum, 62(7), 2127–2137. doi:10.1002/art.27468 [PubMed: 20506317]

Shin JJ, Glickstein LJ, & Steere AC (2007). High levels of inflammatory chemokines and cytokines in joint fluid and synovial tissue throughout the course of antibiotic-refractory Lyme arthritis. Arthritis Rheum, 56(4), 1325–1335. doi:10.1002/art.22441 [PubMed: 17393419]

Sonderegger FL, Ma Y, Maylor-Hagan H, Brewster J, Huang X, Spangrude GJ, … Weis JJ (2012). Localized production of IL-10 suppresses early inflammatory cell infiltration and subsequent development of IFN-gamma-mediated Lyme arthritis. J Immunol, 788(3), 1381–1393. doi: 10.4049/jimmunol.1102359

Steere AC, & Angelis SM (2006). Therapy for Lyme arthritis: strategies for the treatment of antibiotic-refractory arthritis. Arthritis Rheum, 54(10), 3079–3086. doi:10.1002/art.22131 [PubMed: 17009226]

Steere AC, Duray PH, & Butcher EC (1988). Spirochetal antigens and lymphoid cell surface markers in Lyme synovitis. Comparison with rheumatoid synovium and tonsillar lymphoid tissue. Arthritis Rheum, 37(4), 487–495.

Steere AC, Schoen RT, & Taylor E(1987). The clinical evolution of Lyme arthritis. Ann Intern Med, 707(5), 725–731.

Strle K, Shin JJ, Glickstein LJ, & Steere AC (2012). Association of a Toll-like receptor 1 polymorphism with heightened Th1 inflammatory responses and antibiotic-refractory Lyme arthritis. Arthritis Rheum, 64(5), 1497–1507. doi:10.1002/art.34383 [PubMed: 22246581]

Strle K, Sulka KB, Pianta A, Crowley JT, Arvikar SL, Anselmo A, … Steere AC (2017). T-helper 17 cell cytokine responses in Lyme disease correlate with *Borrelia burgdorferi* antibodies during early infection and with autoantibodies late in the illness in patients with antibiotic-refractory Lyme arthritis. Clin Infect Dis, 64(7), 930–938. doi:10.1093/cid/cix002 [PubMed: 28077518]

Sulka KB, Strle K, Crowley JT, Lochhead RB, Anthony R, & Steere AC (2018). Lyme disease-associated IgG4 autoantibodies correlate with synovial pathology in antibiotic-refractory Lyme arthritis. Arthritis Rheumatol, 70(11), 1835–1846. [PubMed: 29790305]

Tran CN, Davis MJ, Tesmer LA, Endres JL, Motyl CD, Smuda C, … Fox DA (2007). Presentation of arthritogenic peptide to antigen-specific T cells by fibroblast-like synoviocytes. Arthritis Rheum, 56(5), 1497–1506. doi:10.1002/art.22573 [PubMed: 17469112]

Tran CN, Thacker SG, Louie DM, Oliver J, White PT, Endres JL, … Fox DA (2008). Interactions of T cells with fibroblast-like synoviocytes: role of the B7 family costimulatory ligand B7-H3. J Immunol, 780(5), 2989–2998.

Viatte S, Plant D, Han B, Fu B, Yarwood A, Thomson W, … Barton A (2015). Association of HLA-DRB1 haplotypes with rheumatoid arthritis severity, mortality, and treatment response. JAMA, 373(16), 1645–1656. doi:10.1001/jama.2015.3435

Vudattu NK, Strle K, Steere AC, & Drouin EE (2013). Dysregulation of CD4+CD25(high) T cells in the synovial fluid of patients with antibiotic-refractory Lyme arthritis. Arthritis Rheum, 65(6), 1643–1653. doi:10.1002/art.37910 [PubMed: 23450683]

Waldburger JM, Suter T, Fontana A, Acha-Orbea H, & Reith W (2001). Selective abrogation of major histocompatibility complex class II expression on extrahematopoietic cells in mice lacking promoter IV of the class II transactivator gene. J Exp Med, 794(4), 393–406.

Wang Q, Drouin EE, Yao C, Zhang J, Huang Y, Leon DR, … Costello CE (2017). Immunogenic HLA-DR-presented self-peptides identified directly from clinical samples of synovial tissue, synovial fluid, or peripheral blood in patients with rheumatoid arthritis or Lyme arthritis. JProteome Res, 76(1), 122–136. doi:10.1021/acs.jproteome.6b00386

Whiteside SK, Snook JP, Ma Y, Sonderegger FL, Fisher C, Petersen C, … Weis JJ (2018). IL-10 deficiency reveals a role for TLR2-dependent bystander activation of T cells in Lyme arthritis. J Immunol, 200(4), 1457–1470. doi:10.4049/jimmunol.1701248 [PubMed: 29330323]

Wormser GP, Dattwyler RJ, Shapiro ED, Halperin JJ, Steere AC, Klempner MS, … Nadelman RB (2006). The clinical assessment, treatment, and prevention of lyme disease, human granulocytic anaplasmosis, and babesiosis: clinical practice guidelines by the Infectious Diseases Society of America. Clin Infect Dis, 43(9), 1089–1134. doi:10.1086/508667 [PubMed: 17029130]

You S, Koh JH, Leng L, Kim WU, & Bucala R (2018). The Tumor-like phenotype of rheumatoid synovium: molecular profiling and prospects for precision medicine. Arthritis Rheumatol, 70(5), 637–652. doi:10.1002/art.40406 [PubMed: 29287304]

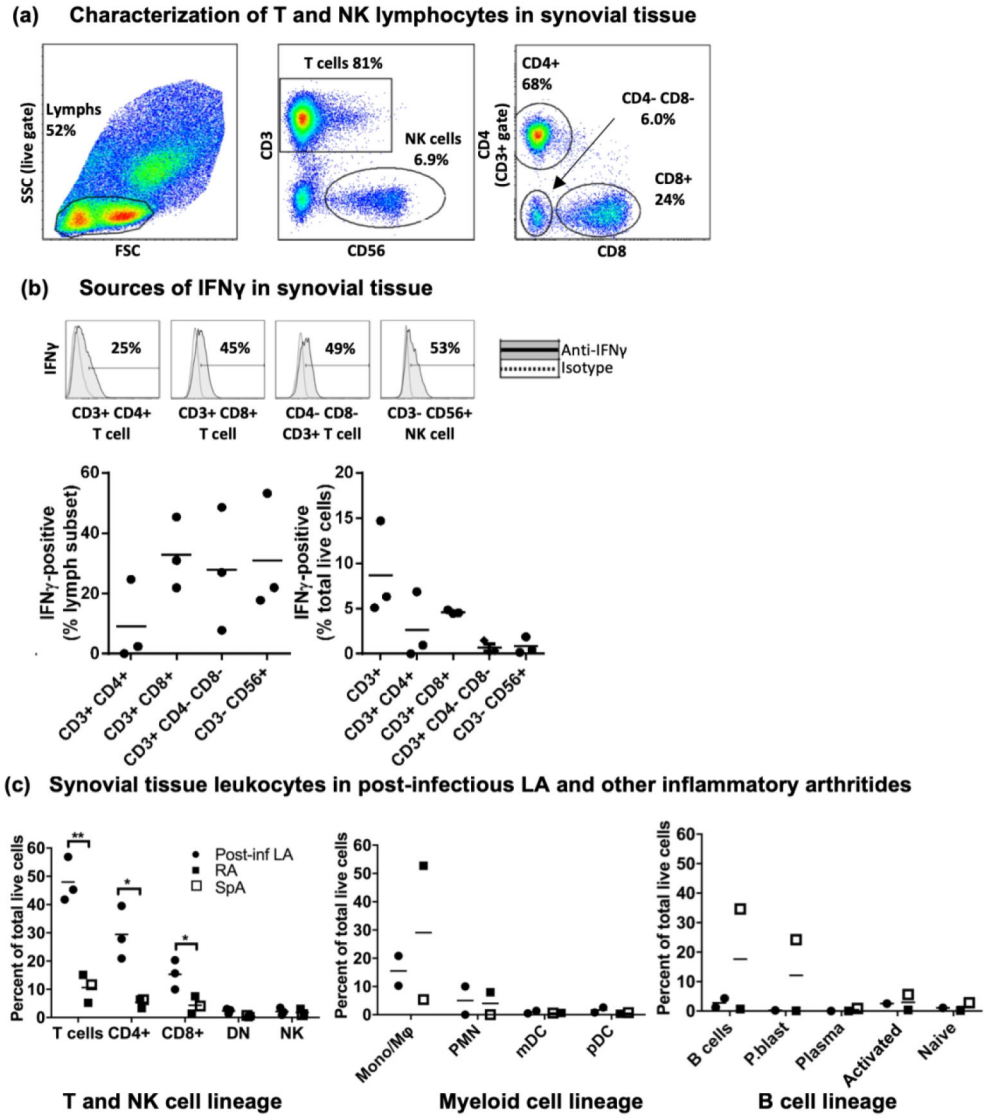

Fig 1: Robust IFNγ production by T cells and NK cells in post-infectious LA synovial tissue.

(a) Characterization of lymphocyte subsets in synovial tissue by flow cytometric analysis collected from 3 patients with post-infectious LA at time of synovectomy. (b) Identification of cellular sources of IFNγ in synovial tissue by intracellular cytokine staining. (c) Comparisons of leukocyte subsets between patients with post-infectious LA vs. other inflammatory arthritis, as a percent of total live cells. Closed circles indicate LA patients, closed squares indicate rheumatoid arthritis (RA) patients, and open squares indicate ankylosing spondylitis (SpA) patient. See Supplemental Figure S1 for myeloid cell and B cell lineage gating strategies. Statistically significant differences between groups were determined by 2-tailed t-test (* $p<0.05$, ** $p<0.01$). Abbreviations: side scatter (SSC), forward scatter (FSC), natural killer cell (NK), CD3+/CD4-/CD8- double-negative T cell (DN), monocyte/macrophage lineage (Mono/Mϕ), polymorphonuclear leukocyte (PMN), myeloid-derived dendritic cells (mDC), plasmacytoid dendritic cell (pDC), plasmablast (P.blast).

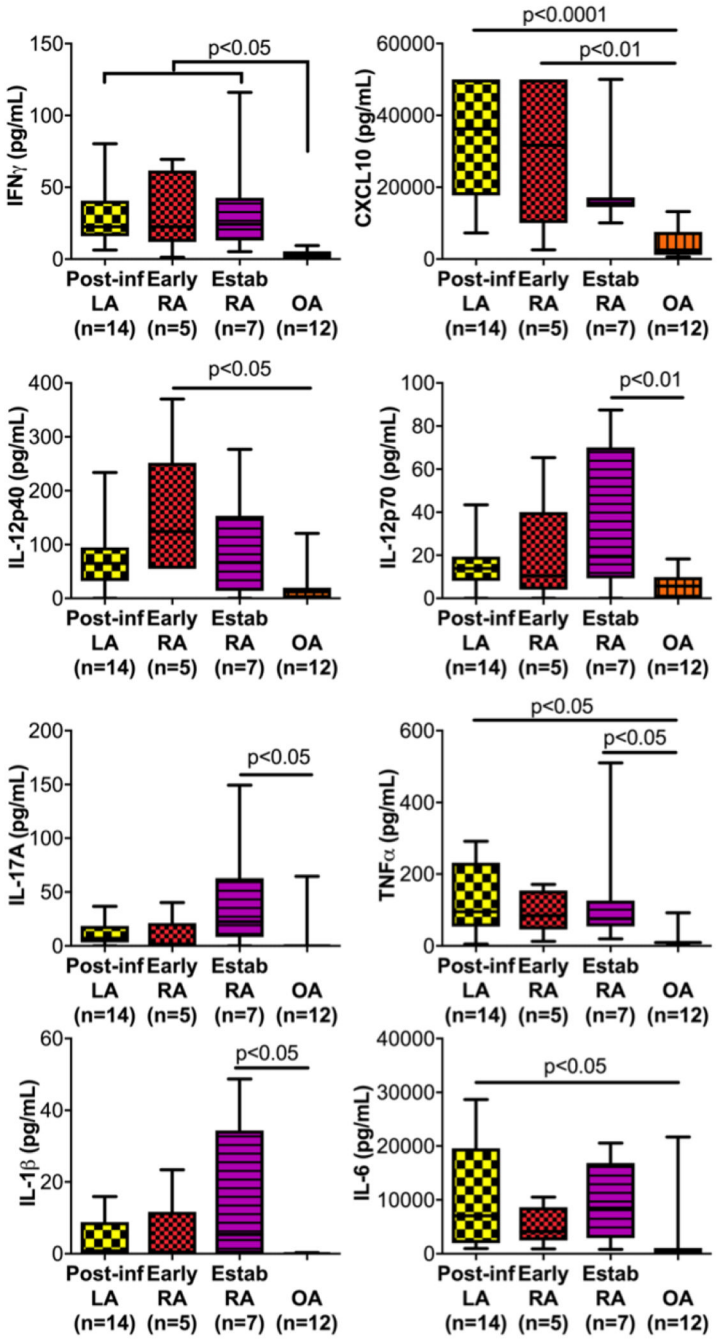

Fig 2: Comparisons of cytokines and chemokines in synovial fluid.

Levels (in pg/ml) of innate and adaptive cytokines and chemokines were assessed in synovial fluid (SF) from 14 patients with post-infectious LA, 5 with early rheumatoid arthritis (RA, <6 months from disease onset), 7 with established RA (>6 months from disease onset), and 12 with osteoarthritis (OA). Statistically significant differences between groups were determined by ANOVA (Tukey's post-hoc), and p-value cutoffs are indicated in the figure.

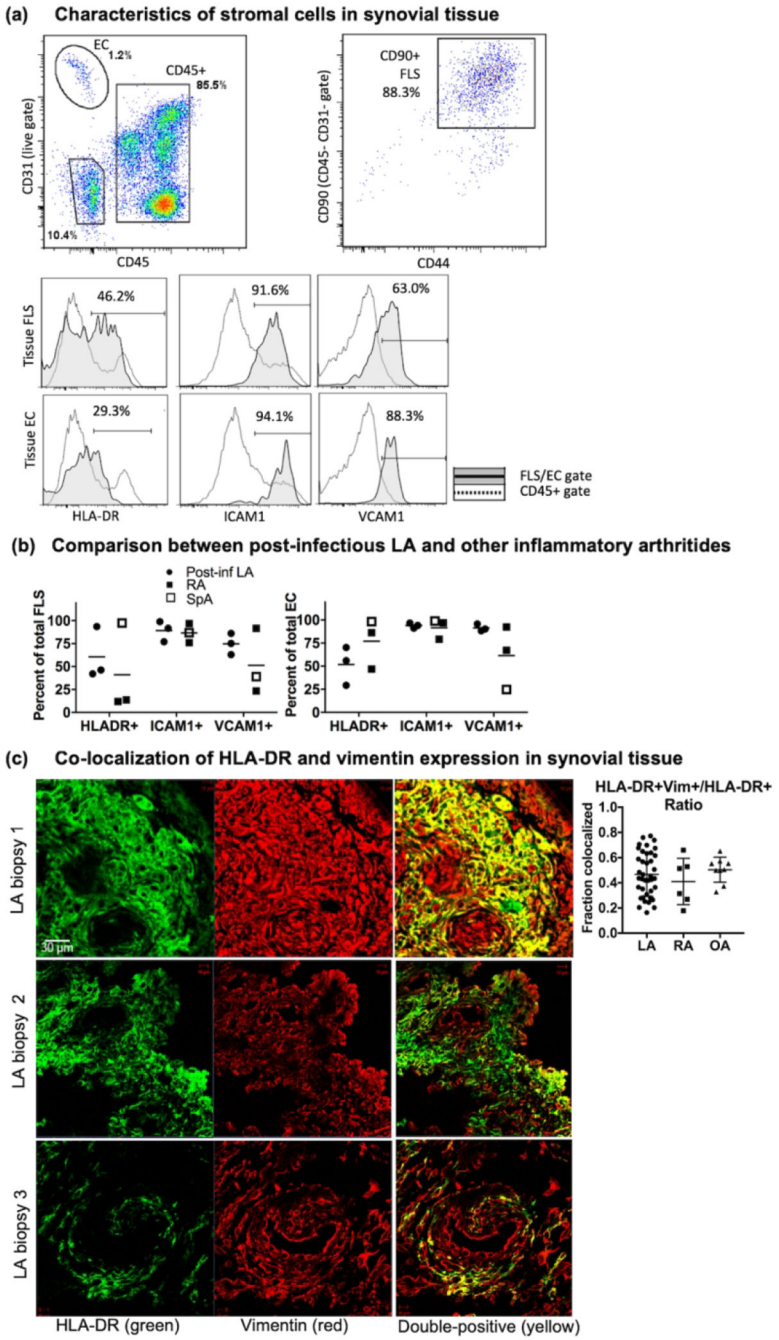

Fig 3: Characterization of stromal cells in synovial tissue.

(a) Gating strategy and phenotypic profiling of endothelial cells (EC) and fibroblast-like synoviocytes (FLS) isolated from freshly digested synovial tissue (top). Staining intensity of HLA-DR, ICAM1, and VCAM1 on FLS and EC (solid line/shaded) were compared with that in the CD45+ gate (dotted line, bottom). (b) Percent of FLS and EC expressing HLA-DR, ICAM1, and VCAM1 in 3 patients with post-infectious LA (closed circles), 2 with rheumatoid arthritis (RA, closed squares), and 1 with ankylosing spondylitis (SpA, open square). (c) Representative images of co-localization of HLADR and vimentin in 3 post-

infectious LA synovial tissue biopsies; and ratio of fluorescence intensity of HLA-DR and vimentin in 3 frames each from biopsies from 13 patients with post-infectious LA, 2 with RA, and 3 with OA.

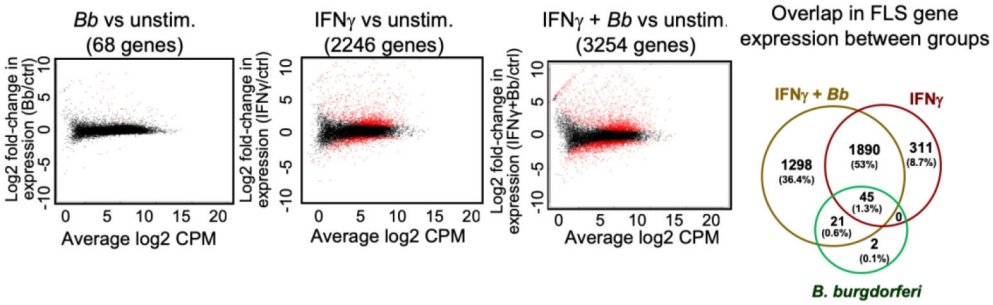

Fig 4: Synergistic effects of *B. burgdorferi* and IFNγ stimulation on FLS gene expression.

Comparison of gene expression from FLS stimulated with *B. burgdorferi*, IFNγ, or both, with red indicating differentially-expressed genes. Overlap in FLS gene expression between groups shown in the Venn diagram (right). Five biological replicates were used for each group, and a differentially-expressed gene was defined as having >2-fold change in gene expression (vs. control) with an adjusted p-value cutoff of 0.05. See Supplemental Table S1 for a complete list of differentially-expressed genes.

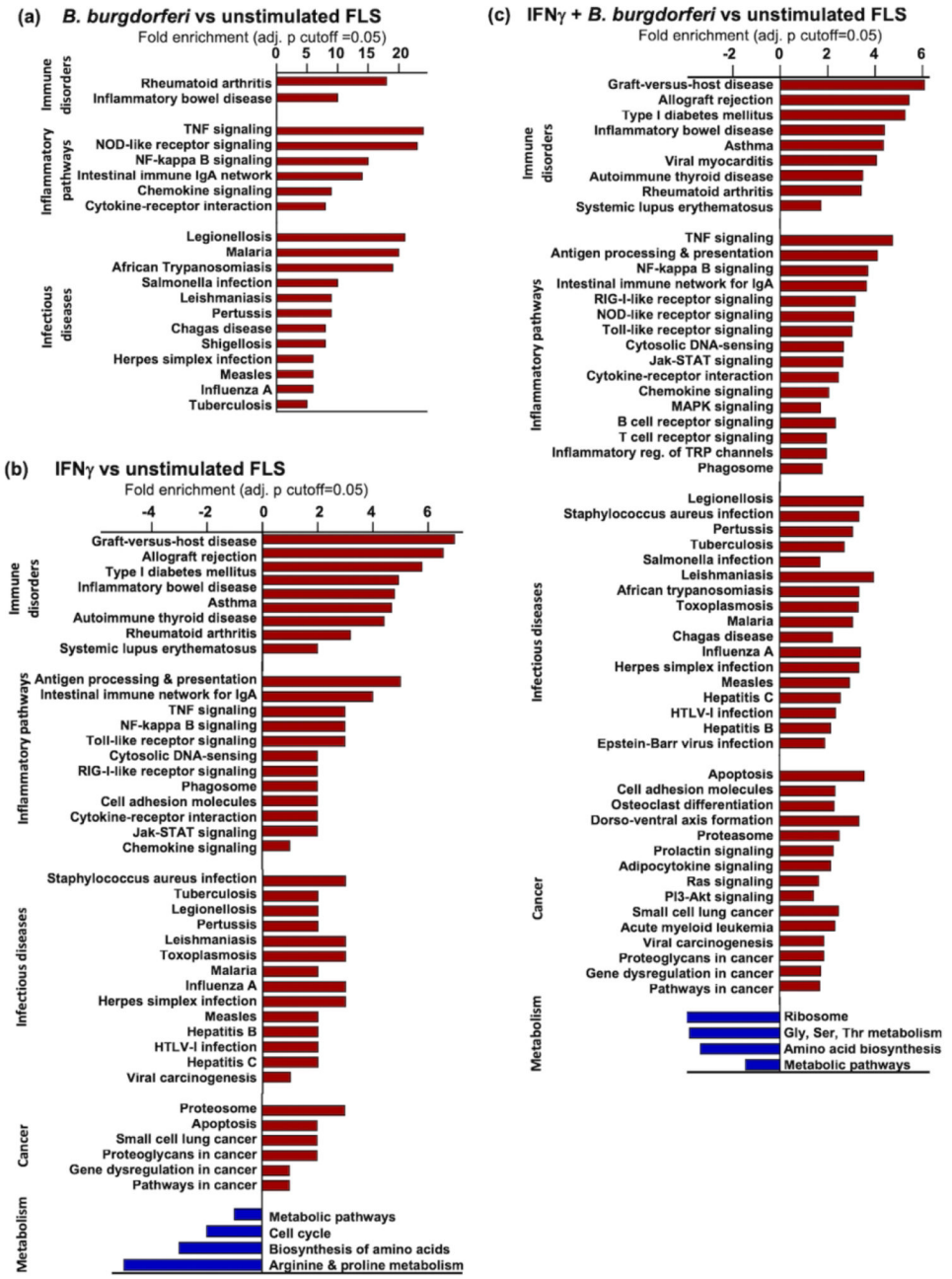

Fig 5: Pathway analysis of differentially expressed genes.

All differentially-expressed genes in FLS stimulated with (a) *B. burgdorferi*, (b) IFNγ, or (c) both were analyzed by KEGG Pathway Analysis to identify gene pathways enriched in stimulated vs. unstimulated cells. FLS from 5 patients were used in each condition (adjusted p-value cutoff=0.05).

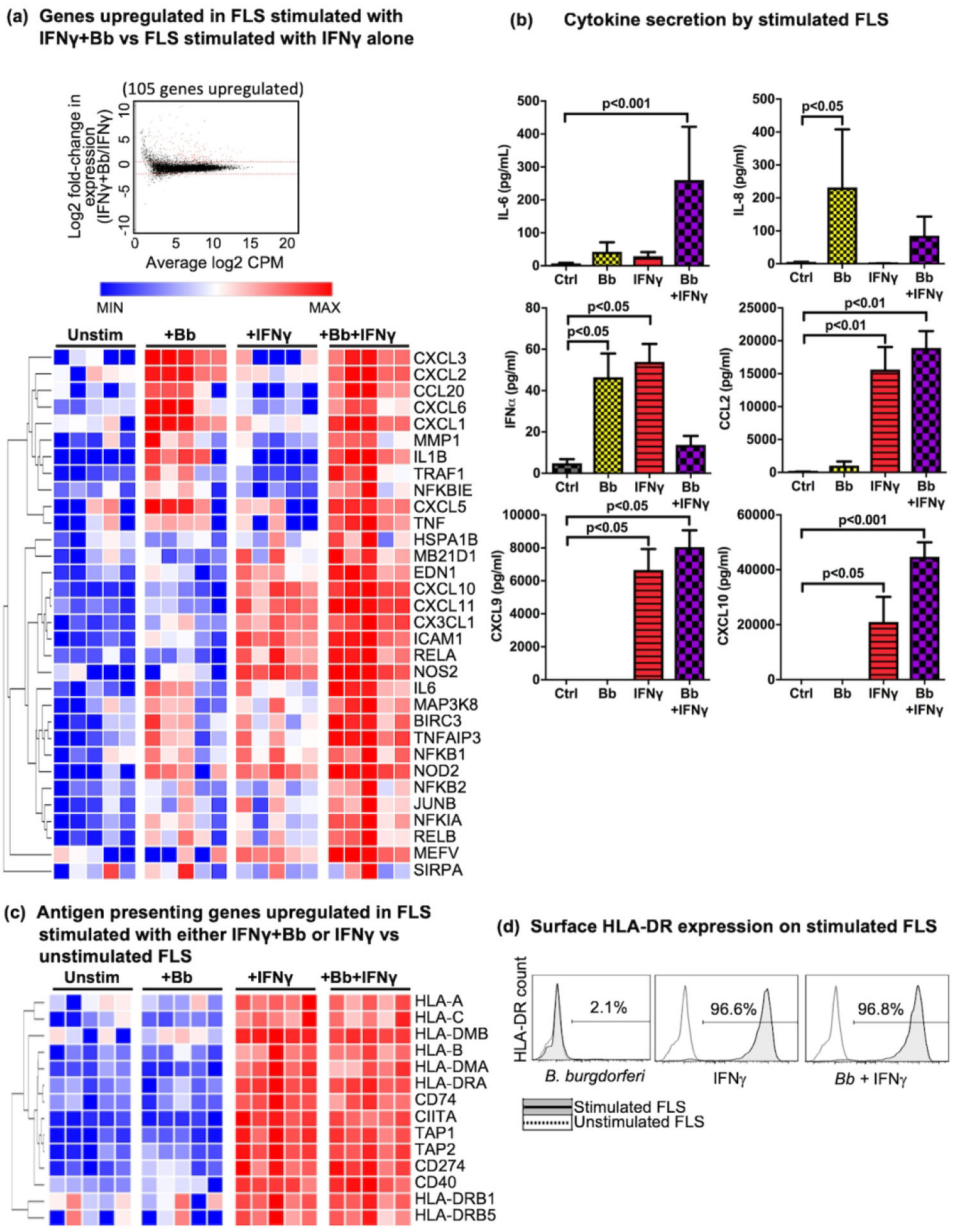

Fig 6: RNA, cytokine, and protein analysis of stimulated FLS.

(a) Comparison of gene expression from FLS stimulated with *B. burgdorferi* +IFNγ or IFNγ alone, with red indicating 105 upregulated genes (see Supplemental Table S1 for complete gene list); and hierarchical clustering analysis of a subset of 32 upregulated genes associated with innate immune activation (i.e., TNF, pathogen recognition receptor (PRR), and NF-kappa B signaling pathways), with minimal gene expression (MIN) in blue, and maximal expression (MAX) in red. (b) Protein levels (in pg/ml) of secreted innate cytokines and chemokines in supernatant of FLS stimulated with *B. burgdorferi*, IFNγ, or *B. burgdorferi* +IFNγ, compared with FLS stimulated with media alone. (c) Hierarchical clustering analysis of a subset of genes associated with antigen processing and presentation expressed in FLS stimulated with IFNγ. (d) Surface expression of HLA-DR molecules on FLS

stimulated with *B. burgdorferi*, IFNγ, or *B. burgdorferi+*IFNγ (solid line/shaded area), compared with FLS stimulated with media alone (dotted line). FLS from 5 patients were used in each experimental condition, and statistically significant differences were determined using Friedman's repeated measures test, with Dunn's correction for multiple comparisons (adjusted p-value cutoffs indicated in figure).